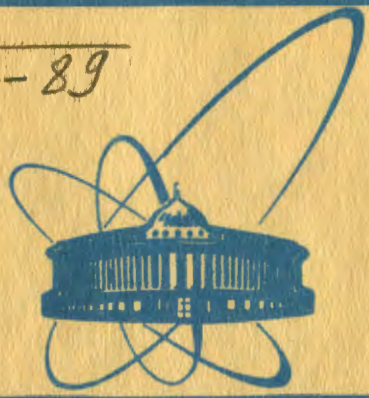

сообщения
объединенного
института
ядерных
исследований
дубна

E1-81-578

Z.Strugalski, K.Miller,* T.Pawlak, W.Peryt,
J.Pluta,* K.Wosińska*

ENERGY-DEPENDENCE OF THE PROTON EMISSION AND PION PRODUCTION INTENSITY DISTRIBUTIONS IN PION-XENON NUCLEUS COLLISIONS

*Institute of Physics of the Warsaw Technical University, Warsaw, Poland.

1981

1. INTRODUCTION

The subject matter of this paper is a presentation of experimental data on correlations of the proton emission process with the pion production process in pion-xenon nucleus collisions at 2.34, 3.50, 5.00 and 8.00 GeV/c projectile momenta. Experiment has been done by means of the 26 litre [1] and 180 litre [2] xenon bubble chambers exposed to pion beams at the Joint Institute for Nuclear Research at Dubna and at the Institute of Experimental and Theoretical Physics at Moscow.

The emitted protons under investigation are of kinetic energy from about 20 to about 400 MeV and correspond roughly to the slow secondaries leaving the so-called gray tracks in nuclear emulsions [3]. In fact, the main constituents of the grey-track-producing particles are fast target protons of kinetic energies from about 40 to about 400 MeV.

The secondary pions registered in our experiments are of any electric charge; the neutral ones are registered and identified in total kinetic energy interval, including zero MeV; the positive pions leave observable tracks if of kinetic energy higher than about zero MeV; the negative ones are observable if of kinetic energy larger than about 10 MeV.

It can be concluded from various experimental data [4-9] that the number of emitted fast target protons is a measure of the nuclear matter layer thickness, measured in the number of nucleons n_N per some area, which an incident hadron has to overcome in colliding with a nucleus at a given impact parameter [10-13].

The information about correlations of the number n_p of emitted fast target protons with the numbers n_π of produced pions might provide, therefore, an important knowledge of the influence of nuclear matter layer thickness on the produced pion average multiplication R_A. This quantity is expressed usually [14] as $R_A = \langle n_\pi \rangle_{hA} / \langle n_\pi \rangle_{hp}$, where $\langle n_\pi \rangle_{hA}$ is the average number of produced pions in a hadron-nucleus collision and $\langle n_\pi \rangle_{hp}$ is the average number of produced pions in the same hadron collision with proton. In the experiments with nuclear photoemulsions instead of $\langle n_\pi \rangle_{hA}$ and $\langle n_\pi \rangle_{hp}$ the average numbers of the shower particles $\langle n_s \rangle$ or of the charged relativistic particles $\langle n_{ch} \rangle$ are often used.

In reviewing experimental data on the n_p-dependences, or n_g-dependences of the $\langle n_\pi \rangle_{hA}$, or of the $\langle n_g \rangle_{hA}$, in hadron - nucleus collisions at energies of 20÷ 200 GeV one can conclude that for a given target nucleus the shapes of these dependences are roughly similar; the dependences are shifted only to the higher values of $\langle n_g \rangle$ with incident hadron energy E_h increasing [7-9]. It is of great importance to see how are such dependences changing at smaller energies E_h. Such information might be useful for the study of hadron behaviour in its passage through the nuclear matter. As we shall see later, the energy dependence of the $\langle n_\pi \rangle - n_p$ and $\langle n_p \rangle - n_\pi$ correlations is evidently seen at incident hadron energies E_h smaller than a few GeV.

2. EXPERIMENT

The pion-xenon nucleus collisions at 2.34, 5 , and 8 GeV/c momenta of incident pions were registered in the 26 litre xenon bubble chamber; the events at 3.5 GeV/c momentum were registered in the 180 litre xenon bubble chamber. The smaller chamber was of the volume 55x29.5x16 cm^3, the 180 litre chamber was of 104x40x40 cm^3 volume. Both the chambers worked without magnetic field.

2.1. Beams and Exposures

During the exposure time no more than five pions were introduced into the chamber, along its length perpendicular to the front wall. The beam pion tracks were parallel and widely spaced within a distance limits of a few centimeters from the chamber axis. Such exposure conditions were of great convenience in studying the pion-xenon nucleus collisions, as we see later.

2.2. Scanning and Measurements

The photographs of the chambers were scanned and rescanned for the pion-xenon nucleus collision events which could occur in a chosen parallelepipedal region of 42x10x10 cm^3 in the bigger chamber and within the region of 27x14x5 cm^3 in the smaller one, both situated coaxially and centred inside the chambers. Any sharp change in the straight line track of any beam pion was considered as an indication that this pion had undergone the interaction with a xenon nucleus. The end or deflection point of any beam pion track we accepted to be the pion-xenon nucleus interaction location. In fact we were able to detect the collision events in which the beam pion

track ends off forming a "star" or not, or deflects at an angle of no less than 2 degrees, in accompaniment or not of any number of negaton-positon pairs produced by gamma quanta outcoming from the interaction place.

The secondary neutral pions of any kinetic energy, including zero, are recorded and identified in our chambers by the simply visible tracks of the negaton-positon conversion pairs and by the observed electron-photon showers created by the gamma quanta appearing in the neutral pion decay process /15/. The minimal energy of the gamma quanta detected with the constant efficiency amounts roughly 5 MeV. The positive pions stopping within the chamber are identified simply by the characteristic track sequence left by the charged secondaries emerged in the decay process. Some difficulties have been met in attempts to identify the negative charged pions stopping inside the chambers and to distinct them from the stopping protons. But, we estimate the portion of such negative pion tracks in the sample of the tracks accepted to be protons. Stopping kaons are identified without difficulties as well . Similarly it was possible to identify hyperons if they decayed inside the chamber. The neutrons which are emitted in the collision process interact with the xenon nuclei frequently leaving characteristic "neutral stars".

Tracks of the lengths larger than about 5 mm are visible well and detectable with the constant efficiency of nearly 100% in both the chambers. To this minimal length corresponds the minimum kinetic energy of the protons of 20 MeV and of the charged pions of roughly 10 MeV. The tracks of the smaller lengths are visible as well but in this case the detection probability is not constant. All tracks left by the particles stopping inside the chambers without visible interaction or decay are accepted to be proton tracks. The portion of the pion-left-tracks in such a sample is estimated to be no more than 2%. The remaining tracks are treated as proton tracks. The protons of kinetic energy from 15 up to about 220 MeV, the secondary pions: the negative charged of kinetic energy from 10 up to about 150 MeV, positive charged of kinetic energy from zero up to about 150 MeV, and the neutral pions of any kinetic energy, including zero MeV, are recorded and identified in such a way with the registration efficiency being near to 100% within the total 4π solid angle in the 180 litre chamber. In the 26 litre chamber such registration and identification efficiency is for protons of kinetic energy from 20 to about 115 MeV, for negative charged pions of kinetic energy from 10 up to about 60 MeV, positive ones from zero up to 100 MeV and for neutral ones of any kinetic energy including zero.

The scanning efficiency for all the pion-xenon nucleus collision events registered in our experiments were better than 99.5%. In nearly 8% of the registered events the tracks of stopped negative pions were indistiguishable from those of proton tracks, it amounts roughly 2% of all the proton tracks. This estimation follows from the studies of nuclear collisions in nuclear emulsions exposed to the negative pion beam /16/. The sample of tracks treated as the proton-left-tracks contains the tracks left by deuterons, tritons and alpha particles as well. It has been estimated that the portion of such tracks amounts no more than a few per cent, if we take into account proton tracks longer than 5 mm. We have estimated that roughly 90% of all emitted protons are stopping inside the chamber.

It is possible to measure the kinetic energies of the stopping protons, of the positive charged pions decaying inside the chambers, using range - energy relation, and of the neutral pions. It is possible as well to measure the emission angles of the protons, charged and neutral pions. The accuracy of the proton energy measurement is, in average, 4% and of the proton emission angle estimation is in average 2 degrees. The accuracy of the charged pions energy estimation is almost the same. The accuracy of the neutral pion energy estimation is, in average, 12% /15/. The accuracy of the pion emission angle estimation, for charged and neutral pions is nearly 1 degree.

The energy and angular characteristics of secondaries we shall not present in this paper, in which the intensities of emitted protons in correlation with the intensities of produced pions are considered only.

3. EXPERIMENTAL DATA

Over 75000 chamber photographs were scanned on which over 15000 pion-xenon collision events were found (see the Table). On the basis of this sample of events various incident pion momentum P_π dependent characteristics of the emitted proton and produced pion intensities were prepared. As the measures of the proton emission intensity the number n_p of emitted protons in any collision event and the average number of protons $\langle n_p \rangle$ in events with a given number n_π of produced pions were used; as the measures of the pion production intensity the number n_π of produced pions in any event and the average number $\langle n_\pi \rangle$ of produced pions in events with a given number n_p of emitted protons were used.

In fig. 1 the P_π -dependence of the average multiplication R_{Xe} of pions inside the xenon nucleus is presented. This quantity is defined as

Table

General Characteristic of Experimental Material Used in this Work

Collision	Chamber	Momentum GeV/c	Number of Photographs Scanned	Number of Collision Events Selected
$Pi^+ - Xe$	26 litre	2.34	20000	6110
$Pi^- - Xe$	180 "	3.5	40000	5487
$Pi^- - Xe$	26 "	5.0	6000	1468
$Pi^- - Xe$	26 "	8.0	9000	1994

$$R_{Xe} = \frac{\langle n_\pi \rangle_{Xe}}{\langle n_\pi \rangle_p}, \qquad (1)$$

where: $\langle n_\pi \rangle_{Xe}$ is the average number of pions - negative, positive and neutral - produced in the pion-xenon collisions at a given incident pion momentum P_π ; $\langle n_\pi \rangle_p$ is the average number of pions of any electric charge produced in the pion-proton collision at the same incident pion energy. In this experiment the values of $\langle n_\pi \rangle_{Xe}$ at $n_p = 0$ have been used instead of the $\langle n_\pi \rangle_p$ in elementary collisions. It can be proved that the n_π distributions in pion-xenon nucleus collisions at $n_p = 0$ are the same as those in the elementary pion-proton collisions.

In fig. 2 n_π distributions in dependence on the incident pion momentum are given. The n_{π^0} distributions of the events under investigation are presented in fig. 3.

Figure 4 presents the n_p distributions of pion-xenon nucleus collision events at various incident pion momenta. The dependence of the average proton multiplicity $\langle n_p \rangle$ on the charged secondary multiplicity n_{ch} for various incident pion momenta is shown in fig. 5.

The n_p-dependences of the average number $\langle n_\pi \rangle$ of produced pions of any electric charge are shown in fig. 6 for various incident hadron momenta P_π .Analogical n_p-dependences of the average numbers $\langle n_{\pi^0} \rangle$ of neutral pions are shown in fig. 7.

The n_p-dependences of the normalized dispersions:

$$Z = \frac{\sqrt{\langle n_\pi^2 \rangle - \langle n_\pi \rangle^2}}{\langle n_\pi \rangle} = \frac{\langle D \rangle}{\langle n_\pi \rangle}$$

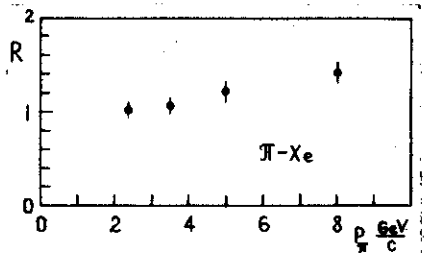

Fig.1. Incident pion momentum P_π -dependence of the produced pion average multiplication R_{Xe} in the pion-xenon collision events at various momenta.

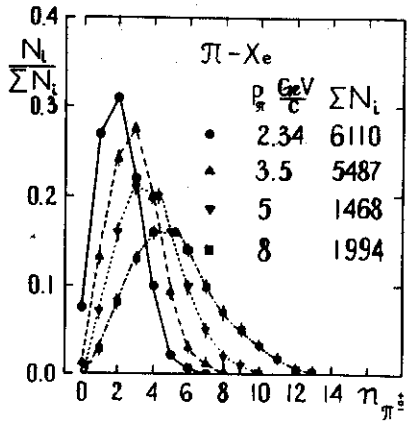

Fig.2. Pion multiplicity, n_π, distributions in pion-xenon collision events at various incident pion momenta P_π. Lines are drawn to guide the eye.

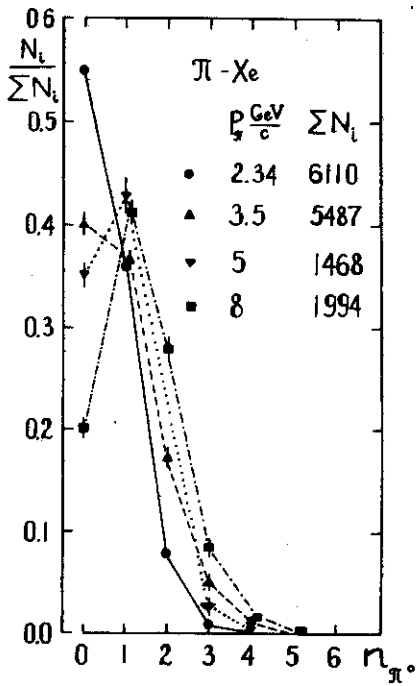

Fig.3. Neutral pion multiplicity, n_{π^0}, distributions in the pion-xenon nucleus collisions at various incident pion momenta P_π. Lines are drawn to guide the eye.

of produced pion numbers n_π, both for any electric charged pions and for neutral ones only, are presented in figs.8 and 9 for various incident pion momenta.

The correlations between number n_π of produced pions, of any electric charge, and the average number $\langle n_p \rangle$ of the proton emitted are shown in fig. 10, for collisions at various incident pion momenta; the dependences of $\langle n_p \rangle$ on the numbers $n_{\pi^\mp}$ of produced negative and positive charged pions are presented in fig. 11. It should be noted that correlation of $n_{\pi^0}^{\mp}$ with $\langle n_p \rangle$ for pion-xenon collisions at 3.5 GeV/c momentum

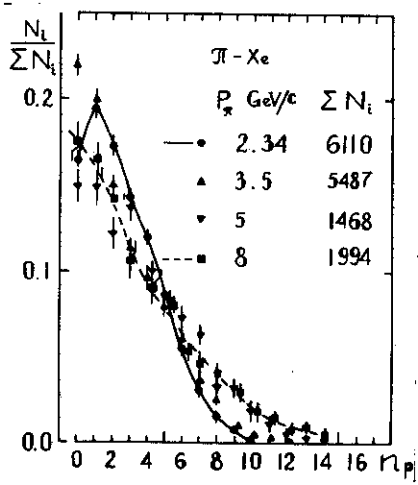

Fig.4. Proton multiplicity, n_p, distributions in the pion-xenon nucleus collision events at various incident pion momenta P_π. Lines are drawn to guide the eye for the collisions at 2.34 GeV/c - solid, and for the collisions at 8 GeV/c - dotted.

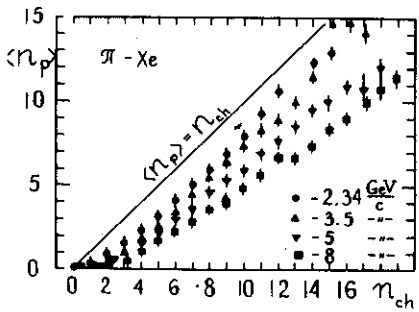

Fig.5. The dependence of the average number of emitted protons $\langle n_p \rangle$ on the charged secondary multiplicity n_{ch} for pion-xenon collisions at various incident pion momenta.

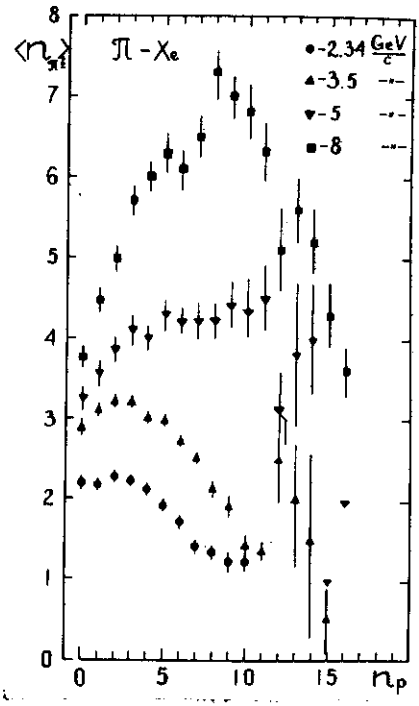

Fig.6. The emitted proton multiplicity n_p-dependence of the average number $\langle n_\pi \rangle$ of pions produced in pion-xenon collisions at various incident pion momenta.

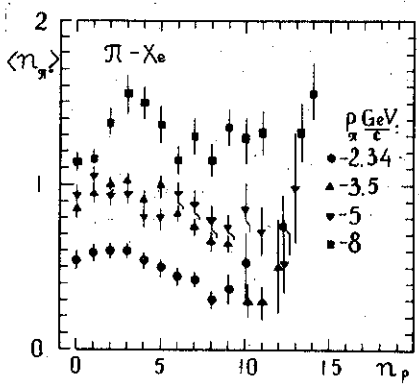

Fig.7. The emitted proton multiplicity n_p-dependence of the average number $\langle n_{\pi^0} \rangle$ of neutral pion produced in pion-xenon collisions at various incident pion momenta P_π.

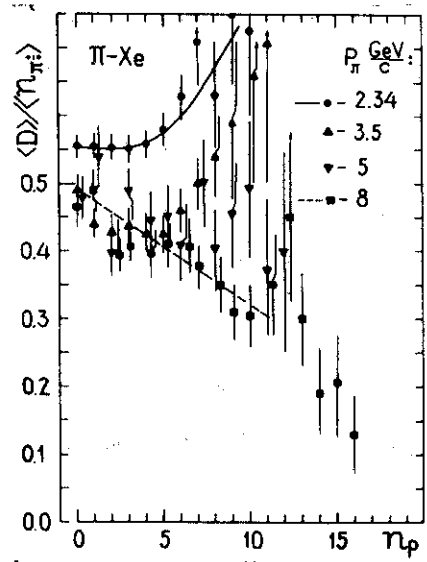

Fig.8. The emitted proton multiplicity n_p-dependences of the normalized dispersion $\langle D \rangle / \langle n_\pi \rangle$ in pion-xenon collisions at various incident pion momenta P_π. Lines are best fitted to the data at P_π = =2.34 GeV/c - solid, and at P_π =8 GeV/c - dotted.

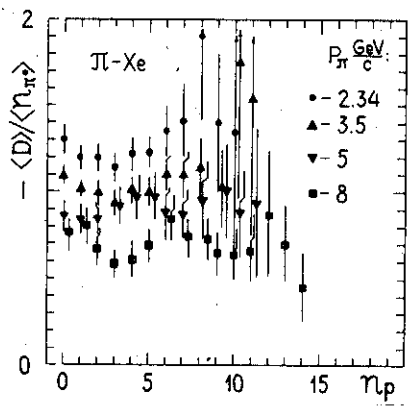

Fig.9. The emitted proton multiplicity n_p-dependences of the normalized dispersion $\langle D \rangle / \langle n_{\pi^0} \rangle$ in pion-xenon collisions at various incident pion momenta P_π.

has been presented in the paper written by Z.Strugalski and J.Pluta /4/ in 1974. In that paper the values of $\langle n_p \rangle$ are higher ; it is because the emitted protons of energies smaller than 20 MeV have been taken into account as well. In that paper it has been emphasized the unusually large number of emitted protons $\langle n_p \rangle$ in which the incident pion is absorbed without pion production, when $n_{\pi^0}^{\mp} = 0$.

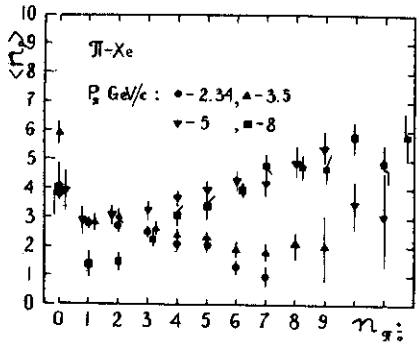

Fig.10. The produced pion multiplicity n_π-dependences of the average multiplicity $\langle n_p \rangle$ of emitted protons in pion-xenon collision events at various incident pion momenta P_π.

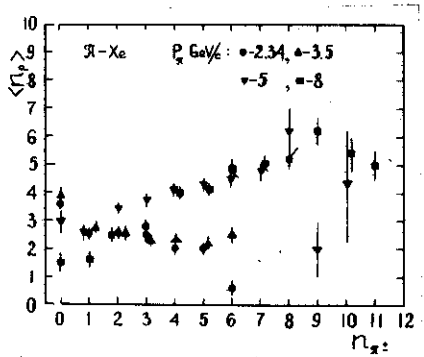

Fig.11. The produced charged pion multiplicity n_π-dependences of the average multiplicities $\langle n_p \rangle$ of emitted protons in pion-xenon collisions at various incident pion momenta P_π.

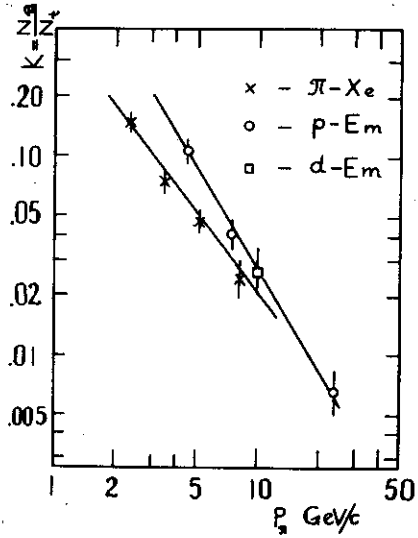

Fig.12. The dependence of the quantity $k = N_a/N_t = aP_\pi^b$ on the incident hadron momentum P_π. The emulsion data are taken from various publications: at 4.5 GeV/c from the work performed in JINR at Dubna[17], at 6.2 and 22.5 GeV/c from the work of Winzeller[18]. Data for d-Em are from the work of Bogatchev et al.[19].

The ratio between the number N_a of events in which incident pions are absorbed in the target nucleus and the total number N_t of all pion-nucleus collision events:

$$k = \frac{N_a}{N_t} \qquad (2)$$

decreases with the incident pion momentum increase. It is observed both for the pion-xenon nucleus and for the proton-nucleus collisions in nuclear photo-emulsions, fig.12; when the proton-nucleus collisions in nuclear emulsions are considered, the number of shower particles n_s is taken instead of the number n_{π^+} of produced pions. The quantity k might be expressed by:

$$k = aP_\pi^b, \qquad (3)$$

where a =0.45 and b =-4/3 for the pion-xenon nucleus collisions, and a =1.1 and b =-5/3 for the proton-nucleus collisions in nuclear emulsions. The point for deuter-nucleus collisions at 9.4 GeV/c momentum[19] lies on the $k-P_\pi$ dependence for the emulsion data.

4. CONCLUSIONS

From the above presented data it follows that:

1. The average multiplication R_{Xe} of the pions produced in the pion-xenon nucleus collisions increases with the incident pion momentum increasing from 2.34 to 8 GeV/c, fig. 1.

2. The emitted protons predominate among the charged secondaries in pion-xenon collisions under consideration, fig. 5. But, the ratio between the number of emitted protons and the number of produced pions decreases with the incident pion momentum increasing within 2.34-8 GeV/c momentum value interval.

3. The n_p-dependence of the average number $\langle n_\pi \rangle$ of the pion produced changes markedly with increasing of the incident pion momentum from 2.34 to 8 GeV/c. The shape of the n_p-dependence at the maximum, in our experiment, incident pion momentum value, P_π =8 GeV/c, is similar to the shapes of such dependences for pion-nucleus[7-9] and proton-nucleus [8] collisions at much higher incident hadron momenta, from 20 to 200 GeV/c. We observe, therefore, the change in the n_p-dependence of the average number of produced pions $\langle n_\pi \rangle$ within the incident pion momentum value interval from roughly 2 up to roughly 5 GeV/c. It should be noted that we observe the dependence of the n_p distribution shapes on the incident pion momentum, as well fig. 4.

4. The n_π-dependence of the average number $\langle n_p \rangle$ of emitted protons changes markedly with the incident pion momentum P_π

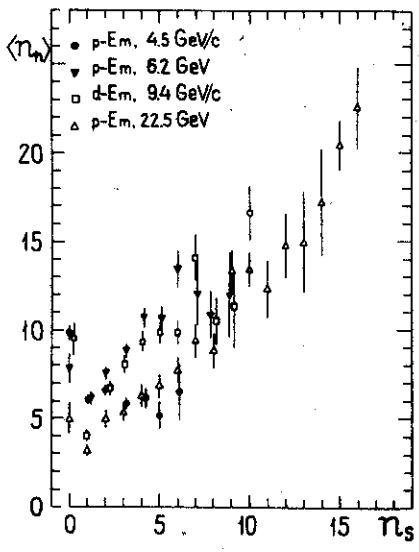

Fig.13. The shower particle multiplicity n_s-dependence of the average number $\langle n_h \rangle$ of heavy particles in proton - nucleus and deuteron-nucleus collisions at various projectile momenta, observed in emulsion experiments. Data are taken from the Dubna - 1980 Collaboration [17], at 4.5; from Winzeller work [18] at 6.2 and 22.5 GeV/c momentum; from the Bogatchov et al. work [19], for d-Em collisions.

variation, fig. 10. Negative correlation is observed at incident pion momenta of 2.34 and 3.5 GeV/c, positive one at momenta of 5 and 8 GeV/c. Similar correlations have been observed in n_s-dependences of the average number of heavy particles $\langle n_h \rangle$ in emulsion experiments, for proton-nucleus collisions at 4.5-22.5 GeV/c momentum [17-19], fig.13. The n_s-dependence of $\langle n_h \rangle$ in deuteron-nucleus collisions at 9.4 GeV/c momentum is similar to the n_s-dependence of $\langle n_h \rangle$ for proton-nucleus collisions, at 6.2 GeV/c, fig. 13.

5. The portion of pion-nucleus collision events in which pions are not present among the secondaries decreases with incident pion momentum increasing as $0.45\ P_\pi^{-1.88}$, fig. 12.

6. The n_p-dependence of the normalized dispersion $\langle D \rangle / \langle n_\pi \rangle$ at incident pion momenta 5.0 and 8 GeV/c are almost the same, within relatively large statistical arrors, as the observed in the Faessler et al. work [9] in pion-nucleus collisions at 20 and 37 GeV/c momenta. But, the dependences at 2.34 and 3.5 GeV/c differ markedly from the other ones, fig. 8. It can be assumed, therefore, that the shape of the n_p-dependence of the normalized dispersion changes with the incident pion momentum only at the values smaller than roughly 3 GeV/c.

REFERENCES

1. Kanarek T.I. et al. Intern. Conf. on High Energy Accelerators and Instrumentation, CERN, 1959, Proceedings, p. 508.
2. Kusnetsov E. et al. Instrumentation and Experimental Technics, (Russian PTE). 1970, 2, p. 56.

3. Powell C.F., Fowler P.H., Perkins D.H. The Study of Elementary Particles by the Photographic Method, Pergamon Press, London-Los Angeles, 1959.
4. Strugalski Z., Pluta J. Journal of Nuclear Physics (Russian), 1974, 27, p. 504.
5. Strugalski Z. et al. JINR, E1-11975, Dubna, 1978.
6. Strugalski Z. et al. JINR, E1-80-39, Dubna, 1980.
7. Babecki J. Report INP No 887/PH, Krakow, 1975; Report INP No 911/PH, Krakow 1975.
8. Andersson B., Otterlund I., Stenlund E. Phys.Lett., 1978, 73B, p. 343.
9. Faessler M.A. et al. Nuclear Phys., 1979, B157, p. 1.
10. Strugalski Z. JINR, E1-80-799, Dubna, 1980.
11. Strugalski Z. JINR, E1-80-216, Dubna, 1980.
12. Pawlak T., Strugalski Z. JINR, E1-81-378, Dubna, 1981.
13. Strugalski Z. JINR, E1-81-154, E1-81-155, E1-81-156, Dubna, 1981.
14. Busza W. In: High Energy Physics and Nuclear Structure, 1975, AIP Conference Proceedings No 26, p. 211; Acta Physica Polonica, 1977, B8, p. 333.
15. Strugalski Z. et al. JINR, E1-5349, Dubna, 1970.
16. Menon M.G.K., Muirhead H., Rochot O., Phil.Mag., 1950, 41, p. 83.
17. Alma-Ata-Bucharest-Dubna-Dushanbe-Kosice-Leningrad-Moscow-Tashkent-Ulan-Bator Collaboration, JINR, P1-13055, Dubna, 1980.
18. Winzeller J. Nuclear Physics, 1965, 69, p. 661.
19. Bogatchev V. et al. JINR, P1-6877, Dubna, 1972.

Received by Publishing Department
on August 25 1981.